

# Segmentation Effect on Inhomogeneity of [110]-Single Crystal Deformation

D V Lychagin<sup>1,2,3</sup>, E A Alfeyrova<sup>1</sup>, V P Nesterenko<sup>1</sup>

<sup>1</sup>National Research Tomsk Polytechnic University, Lenin Avenue, 30, Tomsk, 634050, Russia

<sup>2</sup>National Research Tomsk State University, Lenin Avenue, 36, Tomsk, 634050, Russia

<sup>3</sup>Tomsk State University of Architecture and Building, Solyanaya Square, 2, Tomsk, 634003, Russia

E-mail: [dvl-tomsk@mail.ru](mailto:dvl-tomsk@mail.ru), [katerina525@mail.ru](mailto:katerina525@mail.ru)

**Abstract:** This work presents a detailed analysis of segmentation process in FCC single crystals with compression axis [110] and side faces  $(\bar{1}10)$  and (001) considering effect of octahedral shear crystal-geometry and basic stress concentrators. Sequence of meso-band systems formation on side faces is determined. Macro-segmentation patterns are specified, that are common to the FCC single crystals under investigation. It is proved that rectangular shape of highly compressed crystals, elongated in direction of operating planes, is conditioned by orientation symmetry of compression axis, single crystal side faces and shears directions, which are characteristic for the given orientation. The specified patterns are characteristic only for the samples with initial height-to-width ratio equal to 2. When varying sample height relative to the initial one, segmentation patterns will also vary due to crystal geometry variations.

## 1. Introduction

Deformation topography of FCC metals and alloys varies in relation to stacking-fault energy, crystallographic orientation, deformation degree and conditions [1-5]. Deformation topography differs in different areas of crystal faces and within polycrystalline grains. Crystallite partition into areas with different orientations, number and density of sliding traces occur during plastic deformation. [6]. In each separate area deformation is realized by sliding systems, which differ from those in adjacent areas of the crystal. This phenomenon is known as segmentation. The areas can be regarded as deformation domains. They have both characteristic sliding systems and specific shear procedures. In the latter case, shear domains are studied, where sliding is realized with formation of macro- and meso-clots, macro- and meso-bands of deformation. Clots' distinguishing feature is realization of shears along parallel sliding planes in crystal interior layers. This tendency is enhanced with diminishing of stacking fault energy. Bands deformation is characterized by noticeable distortion of shear traces within them; so deformation mechanism requires separate examination. [6-8].

Magid K.R. et al. [9] has been investigated heterogeneity of copper single crystal deformation. The findings demonstrate shear macro-segmentation in a sample. End and central areas of the crystal have distinctions; however, [9] does not examine this phenomenon in detail.

In polycrystals of FCC metals a single grain is divided into domains with different lattice orientations [10]. Uneven grain deformation causes sub-structural features, which occur on the crystal surface as various deformation topographies. Authors [11] suggests a crystal plasticity model, which considers the single crystal as a stack of domains. Individual domains are deformed homogeneously and correlate velocity and tracing continuity with adjacent domains. All domains co-accommodate behavior of the imposed deformation. The model predicts crystal lattice reorientation, distribution of sliding traces, localization of deformation. Effect of crystal-geometric orientation on segmentation character and type of



deformation topography structural elements FCC single crystal are examined. It is established that segmentation nature relates to crystallographic orientation of both compression axis and side faces. The principal is orientation of octahedral shear planes referred to end apexes and edges, which are areas of higher strains [7, 12].

Thus, segmentation process is an integral part of crystal plastic deformation and has its own characteristics and laws, which are related to internal physical-chemical and crystallographic material parameters and to exposure conditions. Segmentation results in formation of certain topography structural elements on the surface, causes distribution of local deformations and facilitates deformation uniformity. Transfer of Al single crystal segmentation behavior to nickel crystals of the same orientation, as well as examination of their evolution during plastic deformation, are of scientific interest.

This work submits an analysis of segmentation of Al and Ni FCC single crystal with compression axis orientation [110] and lateral faces  $(\bar{1}10)$  and (001); sequences of deformation domains based on crystallography and geometry of octahedral shear as well as a role of basic stress concentrators are examined.

## 2. Materials and methods of research

Object of the study is FCC single crystals with compression axis orientation [110] and lateral faces  $(\bar{1}10)$  and (001). Slipping is performed along crystal systems  $\langle 110 \rangle \{111\}$ . Two octahedral planes, each with two shear directions, are equally loaded for single crystals with compression axis [110]. Schmid factor for uniaxial stress state scheme is equal to 0.41. If sample's height to width ratio is 2, it is possible to distinguish a volume, wherein octahedral shear planes have free exposure to free side faces (Fig. 1). When such crystallographic orientation, shear along octahedral planes is initiated by linear stress concentrator. In the case under examination, there are only two active edges, which are in the plane (001); arrangement of shear planes, relative to base stress concentrators, facilitates each of eight apexes to activate at least one shear system. This crystal-geometric configuration affects formation of topography and segmentation order. Deformation meso-bands being formed on all side faces is a characteristic element of deformation topography of single crystals with compression axis [110]. This paper presents the experimental results obtained from single crystals compressive deformation tests. The deformation was performed with Instron ElectroPuls E10000 testing machine, at rates  $1.4 \cdot 10^{-3} \text{ c}^{-1}$ , at room temperature. To reduce friction force graphite grease was applied. Deformation topography was examined under optical microscope Leica DM 2500P.

## 3. Experimental results and discussion

Figure 1a shows crystallographic images of crystals under examination. Obviously, on parallel edges  $(\bar{1}10)$  two inclined shear traces are to be developed, which will be parallel to exposures of planes (111) and  $(11\bar{1})$ . The shear along these planes, on the faces (001), is to develop a single system of horizontal traces parallel to sample ends. Figure 1b shows 3-D orientation of one octahedral plane family in the single crystal with side faces  $(\bar{1}10)$  and (001). In the central part of the single crystal there is a volume, wherein octahedral shear planes have exposures at all free side faces.

Both octahedral shear plane families share the single crystal into seven volumes:  $A, A_1, D, D_1, E, E_1, K$  (Fig. 1b). Area  $K$  corresponds to the area wherein both octahedral shear plane families have exposures to all free side faces. Areas  $D, D_1$  and  $E, E_1$  correspond to the areas wherein only one octahedral shear plane family has exposure to the face. Uniaxial compression scheme is realized in these areas. The planes, crossing hindered deformation areas with non-uniform multidirectional compression, have exposure to areas  $A$  and  $A_1$ . Therefore, these areas have predicted lower density of shear traces. The face (001) is divided into  $E, K$  and  $E_1$ , wherein horizontal shear traces are to be formed (Fig. 1c). In  $E$  and  $E_1$  they will be predominantly formed according to one principle, and in  $K$  – to two.

The octahedral shear planes geometry is such that one of the planes of each family goes through end edge, being an area of maximum shear stresses [7, 12]. In this case, the shear plane is effectively activated by the linear stress concentrator [7, 12]. Different arrangement of shear domains (marked areas), relatively to testing machine plungers, causes equidistant shear in both directions along the close-packed direction in the central area. In other areas shears will be conducted with testing machine plungers. Now consider macro-segmentation of shear deformation in FCC single crystals with compression axis orientation [110], and faces  $(\bar{1}10)$  and (001).

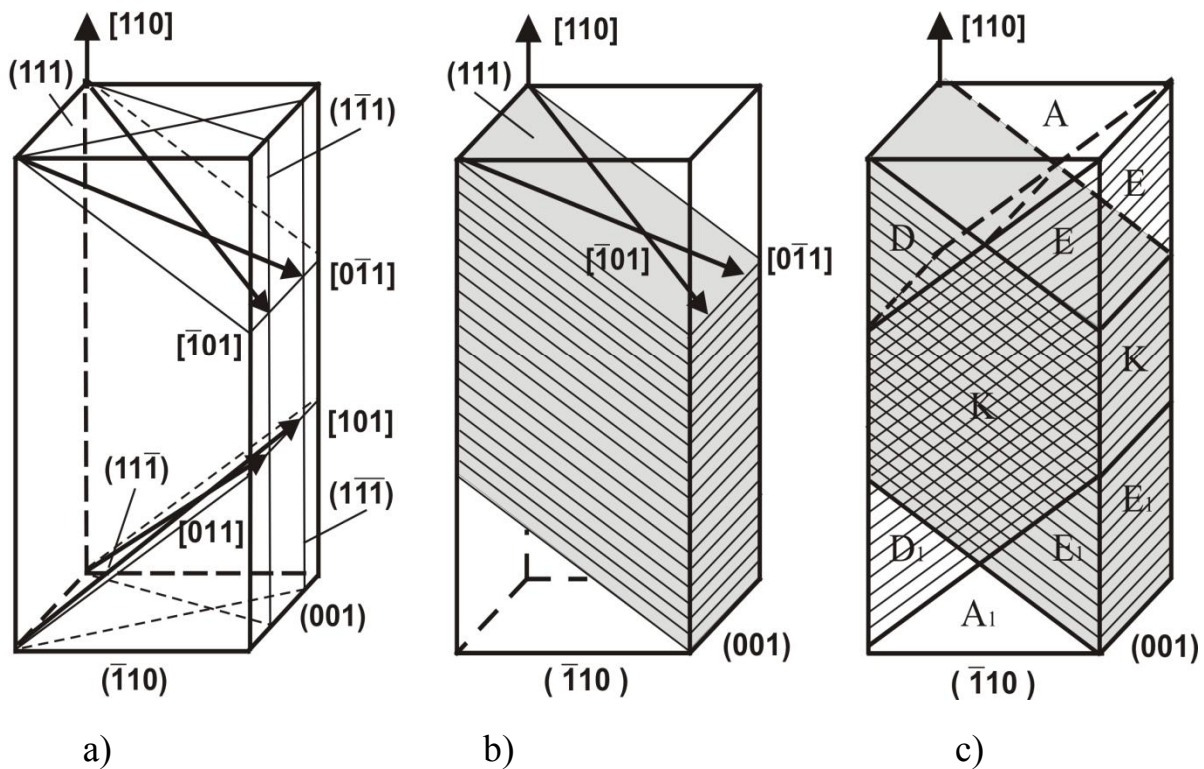


**Figure 1** Crystal-geometry of single crystal with compression axis orientation  $[110]$  and side faces  $(\bar{1}\bar{1}\bar{0})$  and  $(001)$ : plane orientation scheme  $\{111\}$  (a); scheme of one plane family orientation, with exposure to all free edges (b); for two families of equally loaded planes (c) [7]

The octahedral shear planes geometry is such that one of the planes of each family goes through end edge, being an area of maximum shear stresses. In this case, the shear plane is effectively activated by the linear stress concentrator [12]. Different arrangement of shear domains (marked areas), relatively to testing machine plungers, causes equidistant shear in both directions along the close-packed direction in the central area. In other areas shears will be conducted with testing machine plungers. Now consider macro-segmentation of shear deformation in FCC single crystals with compression axis orientation  $[110]$ , and faces  $(\bar{1}\bar{1}\bar{0})$  and  $(001)$ .

Analysis of aluminum and nickel deformation topography shows similarity of shear geometry in the samples being examined. Trace analysis of deformation topography on the side faces proves that most of the traces result from shear planes  $(111)$  and  $(11\bar{1})$ . On faces  $(\bar{1}\bar{1}\bar{0})$  two intersecting trace systems are formed, on faces  $(001)$  - one horizontal trace system. On faces  $(001)$  vertical shear traces are observed in local volumes near the ends. Distribution of shear traces is non-regular both in any system and on the faces. Fig. 2 shows a scheme of shear traces distribution in aluminum single crystal. Nickel single crystals deformation topography has minor differences. Thus, crystallographic factor, which specifies regular geometry of shear planes in the crystal volume, markedly contributes to the segmentation pattern. Fig. 2a is a scheme of primary macro-segmentation of shear deformation. Domains  $A$  and  $A_1$  (Fig. 1c), with the lowest density of active shear planes, are formed in the end areas. There are small areas wherein a macro-level share is not observed. Obviously, in these domains the smallest magnitude of local shear deformations is to be predicted. As noted above, deformation in these areas is hindered because of uniform compression. Trace density is significantly higher near the lower operating plunger if compared with the upper fixed one. Domains  $D$  and  $D_1$ ,  $E$  and  $E_1$  are the areas wherein asymmetrical shear is realized along equally loaded planes. In any domain -  $D$ ,  $D_1$ ,  $E$  and  $E_1$  - the shear along one plane, either  $(111)$  or  $(11\bar{1})$ , prevails. In the central domain  $K$  symmetrical shear occurs along both planes. It is

proved by comparable densities of shear traces along planes  $(111)$  and  $(11\bar{1})$  on the faces  $(\bar{1}10)$ ; aggregate pattern of shear traces in this area is a grid with rhomb or parallelogram elements. The face  $(001)$  is filled with horizontal shear tracks. Morphology of experimentally identified primary domains correlates with that, theoretically predicted by crystallographic analysis. With enhancing of deformation magnitude, additional shear domains occur in aluminum and nickel single crystals (Fig. 2c). From the very beginning of deformation, higher trace density is observed at the boundaries of domains A and A1, at sample apexes. They are marked as separate domains B and B1, C and C1, (Fig. 2a). Such high density of shear traces in these domains is caused by stress concentrations in sample apexes and edges, near testing machine plungers.

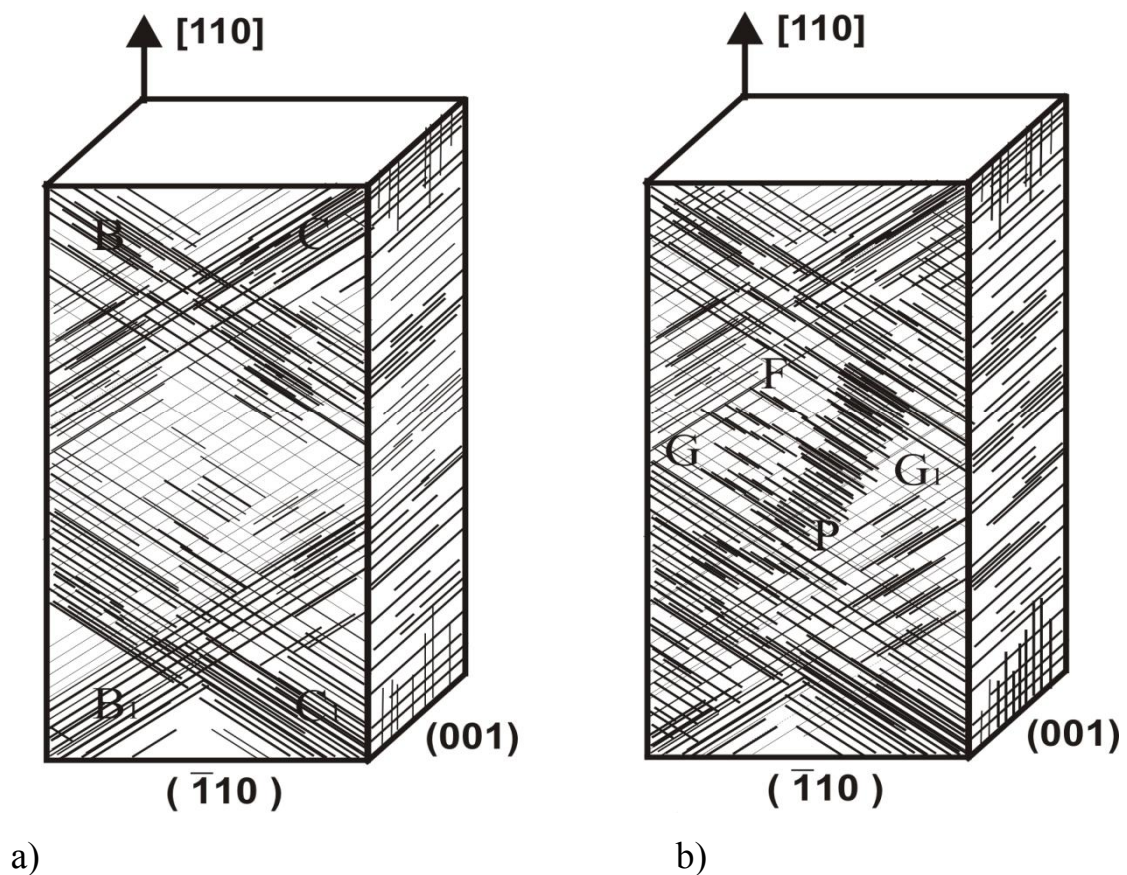


**Figure 2** Shear pattern on faces  $(\bar{1}10)$  and  $(001)$  aluminum single crystal with compression axis orientation  $[110]$  after deformation to  $\varepsilon = 0.03$  (a) and  $\varepsilon = 0.06$  (b) [7]

In the course of plastic deformation, primary domains shear structure evolves and secondary macro-segmentation of deformation develops. Deformation band systems are formed on the face. Deformation band systems are clearly visible in the single crystals of nickel at  $\varepsilon = 0.05$ . In the central domain K four characteristic areas are observed: domains G, G1, F and meso-band system P (fig. 2b). The first three are shear deformation domains, wherein face shear  $(\bar{1}10)$  forms a grid with 0.5 ... 50 mc elements. They are areas of the primary domain K, wherein meso-bands are not formed. The meso-band P is oriented to any face diagonal. Examination of shear pattern on parallel faces  $(\bar{1}10)$  proves that the diagonal band is a volumetric defect. The band is oriented at an angle of approximately  $30^\circ$  to the compression axis within a single crystal volume. Diagonal band boundaries are indistinct; however, if to draw a line through the middle of the band on the face  $(\bar{1}10)$ , this line will be curved relative to the direction  $[\bar{1}10]$ . Another diagonal band, ambidextrous, is less pronounced, i.e. shear symmetry is broken while diagonal bands formation (Fig. 3a).

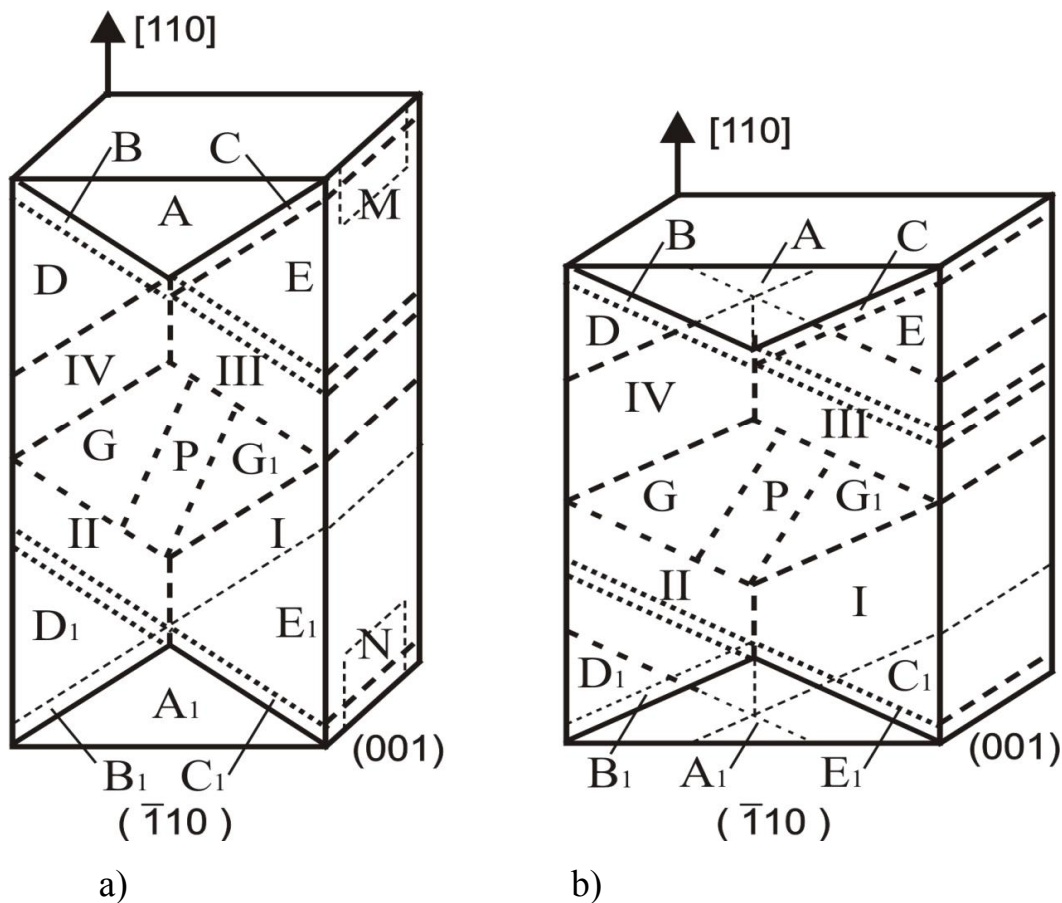


**Figure 3** Scheme of secondary fragmentation in [110]-single crystals: deformation  $\varepsilon \approx 0.05$  (a);  $\varepsilon \approx 0.16$  (b) [7]

Meso-band system developments on side faces  $(\bar{1}10)$  occur in a certain order. They fill area K and adjacent areas  $D$ ,  $D_1$ ,  $E$ , and  $E_1$  in a specific pattern (Fig. 3) in the following sequence: I→II→III→IV. Meso-band systems initiate at the operating plunger (lower end of the sample), and then - at the fixed plunger. These are principal deformation domains; some four - eight domains (two - four at each end on the face (001)), are observed near the plungers of the testing machine. Such domains are formed by shear traces from unloaded octahedron according to uniaxial compression schemes only. These domains are expected when scheme of complex strain state, caused by end friction, is realized. This is verified by joint analysis of traces on all single crystal faces, including the end face. Studies confirm that this phenomenon is a general one. Such aggregate of deformation domains is characteristic only for samples with initial height-to-width ratio equal to 2. When varying sample height, segmentation pattern will also vary.

#### 4. Conclusions

Thus, macro-segmentation regularities are analogous in the investigated FCC single crystals. Orientations of stress axis, single crystal side faces and shear directions are symmetrical, causing initial symmetry of shear spatial organization in single crystals with compression axis [110] and side faces  $(\bar{1}10)$  and (001). With deformation enhancing, shear symmetry is broken to some extent, but prevailing effect of two equally stressed planes continues until large-scale deformation. This results in rectangular shape of highly compressed crystals, elongated in direction of operating planes.

#### Acknowledgements

The reported study was funded by RFBR, according to the research project No. 16-32-60007 mol\_a\_dk.

## References

- [1]. Kuhlmann-Wilsdorf D and Wilsdorf H 1953 *Acta Metallurgica* **1** 4.
- [2]. Robert J. Asaro 1983 *Advances in Applied Mechanics* **23** 1.
- [3]. Hughes D A, Hansen N 1991 *Mater, Sci. Technol.* **7** 544.
- [4]. Gurald Franz, Farid Abed-Meraim, Marcel Berveiller 2013 *International Journal of Plasticity* **48** 1.
- [5]. Zaitsev K, Klimenov V, Loshchilova M, Polovnikov C 2015 IOP Conference Series: Materials Science and Engineering **91** 1 Article number 012056.
- [6]. Bay B, Hansen N, Hughes D A, Kuhlmann-Wilsdorf D 1992 *Acta Metall. Mater.* **40** 2 205.
- [7]. Lychagin D V 2006 *Phys. Mesomech.* **9** 3-4 95.
- [8]. Lychagin D V, Tarasov S Yu, Chumaevskii A V, Alfeyrova E A 2015 *International Journal of Plasticity* **69** 36.
- [9]. Magid K R, Florando J N, Lassila D H, LeBlanc M M, Tamura N and Morris J W 2009 *Philosophical Magazine* **89** 1 77.
- [10]. Kumar M A, Mahesh S 2013 *International Journal of Plasticity* **44** 95.
- [11]. Kumar M A., Mahesh S 2012 *International Journal of Plasticity* **36** 15.
- [12]. Alferova E, Lychagin D, Chernyakov A 2014 *Applied Mechanics and Materials* **682** 485.